Asian Journal of Chemistry; Vol. 27, No. 3 (2015), 902-906

ASIAN JOURNAL OF CHEMISTRY

http://dx.doi.org/10.14233/ajchem.2015.17597

Study on Standard Electrode Potential for 2-Propanethiol Sulfone/2-Propanethiol

Y.Z. SONG[1,*], WEIHAO SONG[2,*], XIAOMENG LV[3], JIMIN XIE[3], A.F. ZHU[1], F.X. ZHU[1] and F.Y. WU[1]

[1]Jiangsu Province Key Laboratory for Chemistry of Low-Dimensional Materials, Jiangsu Key Laboratory for Biomass-Based Energy and Enzyme Technology, School of Chemistry & Chemical Engineering, Huaiyin Normal University, Huai An 223300, P.R. China
[2]Nanjing Foreign Language School Xianlin Campus, Nanjing 210023, P.R. China
[3]School of Chemistry & Chemical Engineering, Jiangsu University, Zhenjiang 212013, P.R. China

*Corresponding authors: Tel: +86 51 783525083; E-mail: songyuanzhi@126.com; mike_sung@sina.com

Received: 12 March 2014; *Accepted*: 17 June 2014; *Published online*: 19 January 2015; AJC-16693

Calculations were performed for 2-propanethiol and 2-propanethiol sulfone. The electrochemical behaviour of 2-propanethiol at gold electrode was investigated by cyclic voltammety and the results showed that the standard electrode potential for 2-propanethiol sulfone/2-propanethiol is 1.073 V, which is consistent with that of 1.083 V at B3LYP/6-31G(d, p)-PCM level. The front orbit theory and Mülliken charges of moleculer explain well on the oxidation of 2-propanethiol in oxidative desulfurization. According to equilibrium theory the experimental equilibrium constant in the oxidative desulfurization system of 2-propanethiol/H_2O_2 is 1.17×10^{48}, which is consistent with the theoretical equilibrium constant of 2.18×10^{48} at B3LYP/6-31++g(d, p)-PCM level, indicating that 2-propanethiol can be oxidized by H_2O_2 and removed from fuel oils.

Keywords: 2-Propanethiol, Standard electrode potential, Oxidative desulfurization.

INTRODUCTION

In recent years, deep desulfurization of fuel oils has attracted increasing attention worldwide because sulfur compounds such as thiols present in oils lead to SO_x emission, which pollutes the air and forms acid rains[1]. There are several techniques such as selective adsorption[2-4], extractive separation[5,6], bio-oxidation[7], hydrodesulfurization[8-10] and oxidative desulfurization[11-15] for removal of sulfur from hydrocarbon fuels. However, the current hydrodesulfurization requires high operating temperature and pressure. It is difficult to remove poly-aromatic sulfur compounds such as benzothiophene, dibenzothiophene, thiophene and their derivative[15]. Oxidative desulfurization was considered as one of the most promising alternative desulfurization processes to obtain ultra low sulfur fuels[2,6-9].

The divalent sulfur can be oxidized by the electrophilic addition reaction of oxygen atoms to form the hexavalent sulfur of sulfones[16]. Fig. 1 illustrates the oxidation reaction scheme for 2-propanethiol.

This paper describes the electrochemical behaviour of 2-propanethiol at a gold electrode, a determination method of standard electrode potential with cyclic voltammetry and the theoretical calculation of standard electrode potential for $PPT_{(O)}/PPT_{(R)}$.

DFT using hybrid functionals has emerged as powerful theoretical method[17-20], we select a B3LYP method at 6-31G (d, p) and 6-31G++ (d, p) level to study the geometries of molecules and the standard electrode potential of half reaction for $PPT_{(O)}/PPT_{(R)}$.

EXPERIMENTAL

All solutions were prepared with distilled-water. $PPT_{(R)}$ was from Aldrich. All reagents were analytical grade.

Electrode preparation: A cylindrical gold electrode, 3 mm in diameter and 50 mm in length, was used for the preparation of the electrode as follows. The gold electrode was prepared for the experiments by polishing to gain a mirror-like appearance, first with fine wet emery papers (grain size 4000) and then with 1 and 0.3 mm alumina slurry on micro cloth pads (Buehler, USA). The gold electrode was activated by holding the potential in 0.1 M H_2SO_4 at +2 V for 5 s and then at -0.35 V for 10 s, followed by potential cycling between -0.35 and +1.5 V at 4 V s^{-1} for 1 min. Finally, the CV characteristic of a clean gold electrode was recorded.

For all electrochemical experiments a CHI660B Electrochemical Analyzer (CHI, USA) was employed. The electrochemical cells consisted of a three electrode, a saturated calomel electrode (SCE), a platinum wire and a gold electrode, were used as the reference, auxiliary and working electrodes, respectively. All cyclo-voltammetric experiments were carried out at 25 °C.

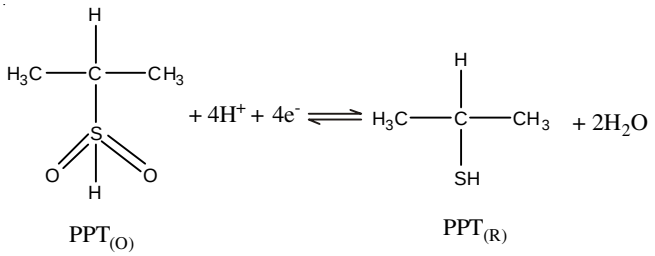

Fig. 1. Reaction scheme for the oxidation of 2-propanethiol

Calculation methods: All the calculations were performed by using the DFT method (B3LYP)[21] with the split-polarized 6-31(d, p) and 6-31G++ (d, p) basis sets, by using the Gaussian 09 suite of programs[22]. Optimized geometries of $PPT_{(O)}$, $PPT_{(R)}$, HBQ, BQ and H_2O in water with no geometrical restriction were calculated with the polarizable continuum model (PCM)[23-25]. All optimized geometries were further examined through vibrational frequency analysis.

RESULTS AND DISCUSSION

Electrochemical investigation of $PPT_{(R)}$ at gold electrode: 2 µL of $PPT_{(R)}$ was added into the surface of gold electrode and the gold electrode insert into 1 M HCl aqueous solution. The cyclic voltammogramm (CVs) of $PPT_{(R)}$ at gold electrode in 1 M HCl aqueous solution are shown in Fig. 2. First CV scan toward positive direction was performed, an oxidation peak of $PPT_{(R)}$ at the gold electrode appeared at 0.831 V (*vs*. SCE), no peaks of 0.831 V for bare gold electrode at gold electrode were found.

Laviron's equation for an irreversible redox couple can be written as[26,27]:

$$E_p = E^{of} + \frac{RT}{\alpha nF}\ln\frac{RTk_s}{\alpha nF} + \frac{RT}{\alpha nF}\ln\nu$$

where α is transfer cofficient, E_p is peak potential, k_s is standard rate constant of the surface reaction, ν is scan rate, E^{of} is conditional potential, n is electron transfer number involved in rate determining step, R is gas constant, T is absolute temperature and F is Faraday constant. When the scan rate is close to zero, E_p equates[26-30] $E^{of}_{PPT_{(O)}/PPT_{(R)}}$.

According to Nernst's equation the peak potential for $PPT_{(O)}$/$PPT_{(R)}$ can be written as $E_p = E^{of}_{PPT_{(O)}/PPT_{(R)}} + \frac{0.059}{4}\log\frac{c^4_{H^+}c_{PPT_{(O)}}}{c_{PPT_{(R)}}}$

If a equation is given as

$$c_{H^+} = c_{PPT_{(O)}} = c_{PPT_{(R)}} = 1\ mol/L$$

then $E_p = E^{of}_{PPT_{(O)}/PPT_{(R)}}$.

when the activities of hydrogen ion are 1 mol/L the conditional potential for $PPT_{(R)}$ and $PPT_{(O)}$ can be written as

$$E^{of}_{PPT_{(O)}/PPT_{(R)}} = E^{\circ}_{PPT_{(O)}/PPT_{(R)}} + \frac{0.059}{4}\log\frac{\gamma_{PPT_{(O)}}\alpha_{PPT_{(R)}}}{\gamma_{PPT_{(R)}}\alpha_{PPT_{(O)}}}$$

where γ and α represent activity coefficient and side reaction coefficient, respectively, E° represents standard electrode potential. Because $PPT_{(R)}$ and $PPT_{(O)}$ are neutral molecules, thus the equations can be written as

$$\gamma_{PPT_{(O)}} = \gamma_{PPT_{(R)}} = 1 \quad \text{and} \quad \alpha_{PPT_{(O)}} = \alpha_{PPT_{(R)}} = 1.$$

Thus the relationship between $E^{of}_{PPT_{(O)}/PPT_{(R)}}$ and $E^{\circ}_{PPT_{(O)}/PPT_{(R)}}$ is given as $E^{of}_{PPT_{(O)}/PPT_{(R)}} = E^{\circ}_{PPT_{(O)}/PPT_{(R)}}$.

The standard electrode potential (E°) *versus* normal hydrogen electrode (NHE) for $PPT_{(O)}$/$PPT_{(R)}$ is calculated as[31]

$$E^{\circ}_{vs,SHE} = E^{\circ}_{vs.SCE} + E_{SCE}(0.242\ V).$$

Therefore, the peak potentials at 10 mV/s for $PPT_{(O)}$/$PPT_{(R)}$ is close to the conditional potentials, the calculated standard potential as above method for $PPT_{(O)}$/$PPT_{(R)}$ is 1.073 V (*vs*. SHE).

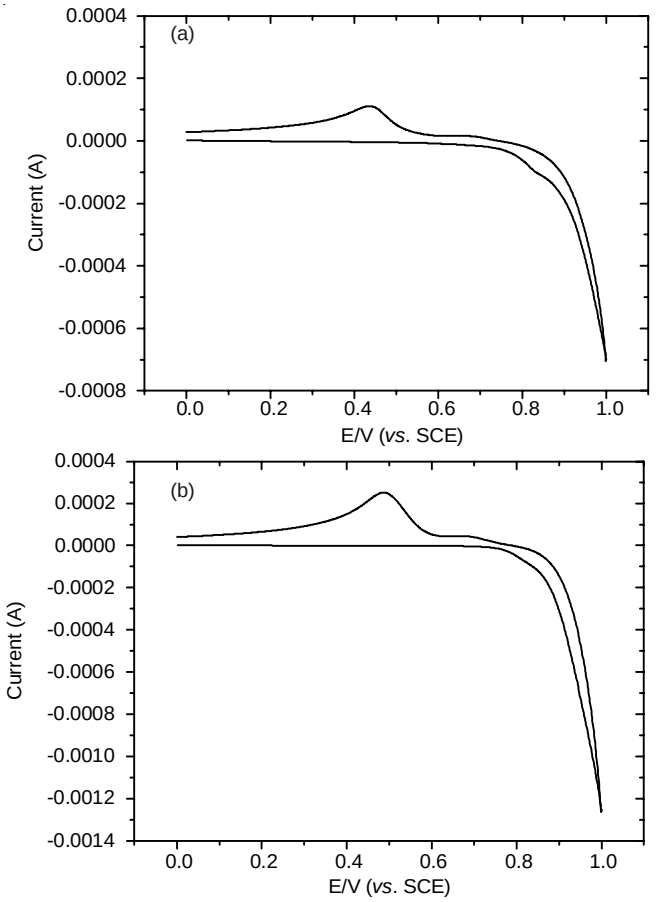

Fig. 2. Cyclic voltammogramms of PPT at gold electrode (a) and gold electrode (b) in 1 M HCl aqueous solution at scan rate of 10 mV/s

Geometry of PPT: The molecular geometries of $PPT_{(O)}$ and $PPT_{(R)}$ are important because the properties are controlled by the geometries, thus the geometries and numeration of atoms in both $PPT_{(R)}$ and $PPT_{(O)}$ are shown in Fig. 3. The selected bond lengths and bond angles of both $PPT_{(R)}$ and $PPT_{(O)}$ optimized at the BLYP/6-31G(d, p)-PCM and B3PP/6-31++g(d, p)-PCM levels are listed in Table-1. It can be seen from Table-1 that the bond lengths and bond angles of the same molecule at BLYP/6-31G (d, p) -PCM level are in a good agreement with the those at B3LYP/6-31++g(d, p)-PCM level.

Eigenvalues of LUMO and HOMO: The highest occupied molecular orbital (HOMO), the lowest unoccupied molecular orbital (LUMO) and energies gap of HOMO and LUMO for $PPT_{(R)}$ and $PPT_{(O)}$ calculated at B3LYP/6-31G (d,

TABLE-1
GEOMETRY PARAMETER OF $PPT_{(R)}$ AND $PPT_{(O)}$

Compound	$PPT_{(R)}$		$PPT_{(O)}$	
Basis sets	6-31G(d, p)	6-31++g(d,p)	6-31G(d, p)	6-31++g(d,p)
Bond length (Å)				
R(1,2)	1.530	1.531	1.530	1.531
R(2,3)	1.528	1.529	1.530	1.531
R(2,4)	1.865	1.865	1.824	1.830
R(4,5)	–	–	1.476	1.481
R(4,6)	–	–	1.476	1.481
Angle (°)				
A(1,2,3)	112.5	112.5	114.1	114.0
A(1,2,4)	107.3	107.4	109.8	109.7
A(3,2,4)	111.8	111.7	109.8	109.7
A(2,4,5)	–	–	109. 5	109.9
A(2,4,6)	–	–	109. 5	109.9
A(5,4,6)	–		119.5	118.8
Dihedral angles (Å)				
D(1,2,4,5)	–	–	-176.8	-176.8
D(1,2,4,6)	–	–	50.5	50.7
D(3,2,4,5)	–	–	-50.5	-50.7
D(3,2,4,6)	–	–	176.8	176.7

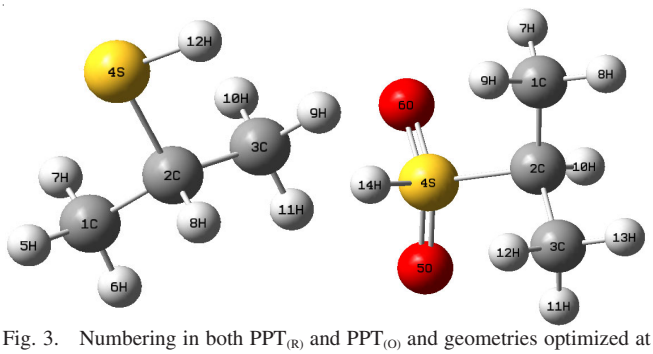

Fig. 3. Numbering in both $PPT_{(R)}$ and $PPT_{(O)}$ and geometries optimized at B3LYP/6-31G++ (d, p)-PCM level

p)-PCM and B3LYP/6-31++g(d, p)-PCM level are shown in Table-2. The eigen values of LUMO and HOMO and its energies gap reflect the chemical activity of molecule. Table-2 shows that the energies of HOMO, the energies of LUMO and the energies gap for $PPT_{(R)}$ are lower than those of $PPT_{(O)}$. Therefore, the HOMO in $PPT_{(R)}$ donates electrons easily and the LUMO in $PPT_{(R)}$ accepts electrons easily. As a result, the oxidation reaction occurs in $PPT_{(R)}$.

TABLE-2
EIGEN VALUES OF LUMO AND HOMO
AND ENERGY GAP OF HOMO AND LUMO

Compound	$PPT_{(O)}$	$PPT_{(R)}$	$PPT_{(O)}$	$PPT_{(R)}$
Basis sets	6-31G(d, p)		6-31++g(d, p)	
E_{HOMO} (eV)	-8.007	-6.564	-8.326	-6.707
E_{LUMO} (eV)	1.431	0.662	-0.252	-0.339
E_{LUMO}- E_{HOMO} (eV)	9.438	7.226	8.578	6.368

From Fig. 4 it can be seen that the electronic density in the HOMO states of $PPT_{(R)}$ and $PPT_{(O)}$ is associated with carbon and sulfur atoms. However, the electronic density in the HOMO states of $PPT_{(R)}$ is associated with p electrons of S and C atoms, which lost electrons easily. The sulfur atoms in HOMO state with p-π and π-π conjugate for $PPT_{(O)}$ lost electrons with difficulty. Therefore, when the oxidation reaction begin, the sulfur atoms in $PPT_{(R)}$ can be oxidized easily.

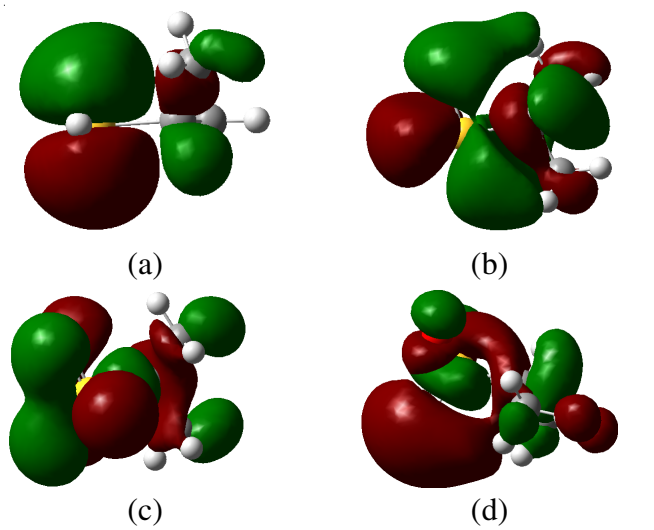

Fig. 4. Electronic density in the HOMO and LUMO states of $PPT_{(R)}$ and $PPT_{(O)}$ calculated at B3LYP/6-31++(d, p)-PCM level: (a)HOMO orbital for $PPT_{(R)}$; (b) LUMO orbital for $PPT_{(R)}$; (c) HOMO orbital for $PPT_{(O)}$; (d) LUMO orbital for $PPT_{(O)}$

Distribution of Mülliken charge and dipole moment: To remove the sulfur compounds in hydrocarbon fuels, the oxidation pruducts of sulfur compounds in oxidative desulfurization system must be solvable in water. The solubility of a compound is controlled by the dipole moments. Thus, the dipole moments of $PPT_{(R)}$ and $PPT_{(O)}$ are discussed here. The totol dipole moments of $PPT_{(R)}$ and $PPT_{(O)}$ at B3LYP/6-31G (d, p) level are 2.3900 and 5.8071 Debye, which are close to those of 2.4728 for $PPT_{(R)}$ and 6.5444 for $PPT_{(O)}$ at B3LYP/6-31G++(d, p) level, respectively, indicating that $PPT_{(R)}$ is weak polar and $PPT_{(O)}$ is strong polar.

The charges of the compound affects on its polarity, thus the charges of atoms are discussed. Mülliken arise from the Mulliken population analysis and provide a means of estimating partial atomic charges, a partial charge is a charge with an absolute value of less than one elementary charge unit (that is, smaller than the charge of the electron). Partial charges are created due to the asymmetric distribution of electrons in chemical bonds. Distribution of Mülliken charges of molecules are shown in Table 3. From Table 3 the Mülliken charges of S in $PPT_{(O)}$ are more positive than that of S in $PPT_{(R)}$ and the Mülliken charges of O_{14} and O_{15} in $PPT_{(O)}$ are markedly more negative than the other atoms. Hence, $PPT_{(O)}$ is soluble in aqueous solution and separable from oil easily. However, $PPT_{(R)}$ is water-insolube, the oxidation reaction for $PPT_{(R)}$ in aqueous solution occurs with difficulty, so a carrier must be presented in oxidative desulfurization for transferring $PPT_{(R)}$ from oil to aqueous solution.

Calculation of standard electrode potential: The theoretical calculation of standard electrode potential for $PPT_{(O)}/PPT_{(R)}$ *versus* benzoquinone/hydroquinone ($E^{\circ}_{BQ/HBQ}$ = 0.699 V)[31] can be designed as

$$PPT_{(R),\,solu} - 4e^- - 4H^+ + 2H_2O_{solu} \rightleftharpoons PPT_{(O),\,solu}$$

$$HBQ_{solu} - 2e - 2H^+ \rightleftharpoons BQ_{solu}$$

where $PPT_{(O),solu}$, $PPT_{(R),solu}$, BQ_{solu}, H_2BQ_{solu} represent 2-propanethiol sulfone, 2-propanethiol, benzoquinone and hydroquinone in water, respectively, then a reaction is given as:

TABLE-4
CALCULATED THERMOCHEMISTRY VALUES, THE ΔrG_{SOLU}(298.15 K, 1 ATM) AND STANDARD ELECTRODE POTENTIAL (E°)

Compound	$PPTH_{(R)}$		$PPTH_{(O)}$		H_2BQ		BQ		H_2O	
Basis set	6-31G(d, p)	6-31++g(d,p)	6-31G(d, p)	6-31++g(d,p)	6-31G(d, p)	6-31++g(d,p)	6-31G(d, p)	6-31++g(d,p)	6-31G(d, p)	6-31++g(d,p)
G_{solu} (Hartree)	-517.270884	-517.276491	-667.644378	-667.662501	-382.627684	-382.650561	-381.410899	-381.432291	-76.423076	-76.439470
G_{solu}(KJ/mol)	-102.626	-148.052	–	–	–	–	–	–	–	–
E° (V)	0.965	1.083	–	–	–	–	–	–	–	–

TABLE-3
DISTRIBUTION OF MÜLLIKEN CHARGE

Compound	$PPT_{(O)}$	$PPT_{(R)}$	$PPT_{(O)}$	$PPT_{(R)}$
Basis sets	6-31g(d, p)		6-31++g(d, p)	
C_1	0.08318	0.04614	-0.01244	-0.01932
C_2	-0.10282	-0.05044	0.132353	0.15839
C_3	0.08317	0.04675	-0.01253	-0.07988
S_4	1.07286	-0.04245	1.19274	-0.05920
O_5	-0.56820	–	-0.65011	–
O_6	-0.56819	–	-0.65002	–

$$PPT_{(O)solu} + 2HBQ_{solu} = PPT_{(R),solu} + 2H_2O_{solu} + 2BQ_{solu}$$

The transformed Gibbs energy above reaction is written as

$$\Delta rG_{solu} = \Sigma[G_{solu,\,product}]_i - [G_{solu,\,reactant}]_i$$

where G_{solu} represents Gibbs free energies of products and reactants in water at 298.15 K and 1 atm, which can be calculated from Gaussian 09 package and ΔrG_{solu} represent the standard transformed Gibbs energy of reaction in water.

The standard electrode potential (E°) of half reaction for $PPT_{(O)}/PPT_{(R)}$ is calculated as

$$\Delta rG_{solu}(298.15\ K,\ 1\ atm) = -nF(E^{\circ}_{PPT_{(O)}/PPT_{(R)}} - E^{\circ}_{BQ/HBQ})$$

The calculated thermochemistry values of this reaction from Gaussian 09 are shown in Table-4, the ΔrG(298.15 K) for the redox reaction and standard electrode potentials (E°) of half reaction for $PPT_{(O)}$ and $PPT_{(R)}$ are also calculated. From Table-4 the transformed Gibbs energies of reaction and standard potential of 0.965 V calculated at B3LYP/6-31g (d, p)-PCM level are in agreement with that calculated at B3LYP/6-31G++(d, p)-PCM level and the predicted standard electrode potentials of 1.083 V at B3LYP/6-31++g(d, p)-PCM level is more close to the experimental values of 1.073V for PPT(O)/$PPT_{(R)}$ in 1 M HCl aqueous solution.

Equilibrium constant: The H_2O_2 as an oxidizer is present in current oxidative desulfurization system; therefore, the redox reaction is designed as below

$$2H_2O_2 + PPT_{(R)} \rightleftharpoons 2H_2O + PPT_{(O)}$$

$E^{\circ}_{H_2O_2/H_2O} = 1.77$, the equilibrium constant (K) of above reaction[31] is calculated as

$$\log K = \frac{n(E^{\circ}_{H_2O_2/H_2O} - E^{\circ}_{PPT_{(O)}/PPT_{(R)}})}{0.059}\ (25\ ^{\circ}C,\ 1\ atm).$$

Thus, the experimental equilibrium constant can be calculated to be 1.80×10^{47}, while the theoretical equilibrium constant can be calculated to be 3.79×10^{54} at B3LYP/6-31g (d, p) level and 3.78×10^{46} B3LYP/6-31++g(d, p)-PCM level, respectively.

The results indicated that the concentration of $PPT_{(R)}$ in water is very low. Therefore, $PPT_{(R)}$ can be oxidized by H_2O_2 and removed from fuel oil. The $PPT_{(R)}$ in oil is controlled by not only the concentration of H_2O_2 and $PPT_{(O)}$, but also the concentration of $PPT_{(R)}$ in water, therefore the catalyst and temperature in oxidative desulfurization system are also important factor.

Conclusion

The geometries of $PPT_{(O)}$ and $PPT_{(R)}$ are optimized at B3LYP/6-31G (d, p)-PCM and B3LYP / 6-31G++(d, p)-PCM level, respectively. The predicted standard electrode potentials of 1.083V at B3LYP/6-31G++(d, p)-PCM level) are in agreement with experimental date (1.073 V for $PPT_{(R)}$ in 1 M HCl aqueous solution). This method is very useful to predict unknown standard potential of compounds because theoretical method is very simple and low-cost. The front orbit theory and Mülliken charges of moleculer explain well on the electrochemical behaviour of cyclo-voltammetry for $PPT_{(R)}$ at gold electrode. PPT can be oxidized by H_2O_2 and removed from fuel oils.

ACKNOWLEDGEMENTS

The authors gratefully acknowledge the financial support of National Science Foundation of China (grant No. 51175245), the Open Science Foundation for Jiangsu Province Key Laboratory for Chemistry of Low-Dimentional Materials (grant no. JSKC13126), the Open Science Foundation for Jiangsu Key Laboratory for Biomass-based Energy and Enzyme Technology (grant No. JSBEET1207) and the Science Foundation for Huaiyin Normal University (grant No. 11HSGJBZ13).

REFERENCES

1. J. Winebrake, J.J. Corbett, E.H. Green, A. Lauer and V. Eyring, *Environ. Sci. Technol*., **43**, 4776 (2009).
2. M. Yaseen, M. Shakirullah, I. Ahmad, A.U. Rahman, F.U. Rahman, M. Usman and R. Razzaq, *J. Fuel Chem. Technol*., **40**, 714 (2012).
3. V.M. Kogan, P.A. Nikulshin and N.N. Rozhdestvenskaya, *Fuel*, **100**, 2 (2012).
4. S.A. Ali, S. Ahmed, K.W. Ahmed and M.A. Al-Saleh, *Fuel Process. Technol*., **98**, 39 (2012).
5. W. Azelee, W.A. Bakar, R. Ali, A.A.A. Kadir and W.N.A.W. Mokhtar, *Fuel Process. Technol.*, **101**, 78 (2012).
6. J. Bu, G. Loh, C.G. Gwie, S. Dewiyanti, M. Tasrif and A. Borgna, *Chem. Eng. J*., **166**, 207 (2011).
7. K.K. Sarda, A. Bhandari, K.K. Pant and S. Jain, *Fuel*, **93**, 86 (2012).
8. M. Seredych, C.T. Wu, P. Brender, C.O. Ania, C. Vix-Guterl and T.J. Bandosz, *Fuel*, **92**, 318 (2012).
9. X. Chen, D. Song, C. Asumana and G. Yu, *J. Mol. Catal. Chem*., **359**, 8 (2012).
10. C.D. Wilfred, C.F. Kiat, Z. Man, M.A. Bustam, M.I.M. Mutalib and C.Z. Phak, *Fuel Process. Technol*., **93**, 85 (2012).
11. I. Sharafutdinov, D. Stratiev, I. Shishkova, R. Dinkov, A. Batchvarov, P. Petkov and N. Rudnev, *Fuel*, **96**, 556 (2012).
12. G. Yu, J. Zhao, D. Song, C. Asumana, X. Zhang and X. Chen, *Ind. Eng. Chem. Res*., **50**, 11690 (2011).
13. W.Y. Liu, Z.L. Lei and J.K. Wang, *Energy Fuels*, **15**, 38 (2001).

14. P. Agarwal and D.K. Sharma, *Energy Fuels*, **24**, 518 (2010).
15. J. Wang, D. Zhao and K. Li, *Energy Fuels*, **24**, 2527 (2010).
16. H. Zhang, J. Gao, H. Meng and C.X. Li, *Ind. Eng. Chem. Res*., **51**, 6658 (2012).
17. Y. Song, L. Zhang, HuiZhong, D. Shi, J. Xie and G. Zhao, *Spectrochim. Acta A*, **70**, 943 (2008).
18. Y.Z. Song, A.F. Zhu, J.X. Lv, G.X. Gong, J.M. Xie, J.F. Zhou, Y. Ye and X.D. Zhong, *Spectrochim. Acta A*, **73**, 96 (2009).
19. D.Q. Shi, X.F. Zhu and Y.Z. Song, *Spectrochim. Acta A*, **71**, 1011 (2008).
20. Y.Z. Song, *Can. J. Chem*., **88**, 676 (2010).
21. A.D. Becke, *J. Chem. Phys*., **98**, 5648 (1993).
22. M.J. Frisch, G.W. Trucks, H.B. Schlegel, G.E. Scuseria, M.A. Robb, J.R. Cheeseman, G. Scalmani, V. Barone, B. Mennucci, G.A. Petersson, H. Nakatsuji, M. Caricato, X. Li, H.P. Hratchian, A.F. Izmaylov, J. Bloino, G. Zheng, J.L. Sonnenberg, M. Hada, M. Ehara, K. Toyota, R. Fukuda, J. Hasegawa, M. Ishida, T. Nakajima, Y. Honda, O. Kitao, H. Nakai, T. Vreven, J.A. Montgomery Jr., J.E. Peralta, F. Ogliaro, M. Bearpark, J.J. Heyd, E. Brothers, K.N. Kudin, V.N. Staroverov, R. Kobayashi, J. Normand, K. Raghavachari, A. Rendell, J.C. Burant, S.S. Iyengar, J. Tomasi, M. Cossi, N. Rega, J.M. Millam, M. Klene, J.E. Knox, J.B. Cross, V. Bakken, C. Adamo, J. Jaramillo, R. Gomperts, R.E. Stratmann, O. Yazyev, A.J. Austin, R. Cammi, C. Pomelli, J.W. Ochterski, R.L. Martin, K. Morokuma, V.G. Zakrzewski, G.A. Voth, P. Salvador, J.J. Dannenberg, S. Dapprich, A.D. Daniels, O. Farkas, J.B. Foresman, J.V. Ortiz, J. Cioslowski and D.J. Fox, Gaussian, Inc., Wallingford CT (2009).
23. R. Bonaccorsi, R. Cimiraglia and J. Tomasi, *Comput. Chem*., **4**, 567 (1983).
24. J.L. Pascualahuir, E. Silla, J. Tomasi and R.J. Bonaccorsi, *Comput. Chem*., **8**, 778 (1987).
25. S. Miertus, E. Scrocco and J. Tomasi, *Chem. Phys*., **55**, 117 (1981).
26. E. Laviron, *J. Electroanal. Chem*., **52**, 355 (1974).
27. E. Laviron, *J. Electroanal. Chem*., **101**, 19 (1979).
28. F. Wang, Y. Wu, J. Liu and B. Ye, *Electrochim. Acta*, **54**, 1408 (2009).
29. F. Wang, Y. Xu, J. Zhao and S. Hu, *Bioelectrochemistry*, **70**, 356 (2007).
30. Y.H. Wu, X.B. Ji and S.S. Hu, *Bioelectrochemistry*, **64**, 91 (2004).
31. D. Dobos, Electrochemical Data, A Handbook for Electrochemists in Industry and Universities; Elsevier Scientific Publishing Company: Amsterdam-Oxford, New York, pp. 88-89 (1975).